Usefulness of Multidetector-row CT in the Evaluation of Reperfused Myocardial Infarction in a Rabbit Model

Jong Min Park, MD
Yeon Hyeon Choe, MD
Samuel Chang, MD
Yon Mi Sung, MD
Seok Seon Kang, MD
Min Joo Kim, MD
Boo-Kyung Han, MD
Sang-Hee Choi, MD

Index terms:
Animals
Computed tomography (CT), multidetector-row,
Computed tomography (CT), helical technology,
Myocardium, infarction,
Myocardium, CT
Heart, CT

Korean J Radiol 2004;5:19-24
Received September 29, 2003; accepted after revision January 26, 2004.

Department of Radiology and Center for Imaging Science, Samsung Medical Center, Sungkyunkwan University School of Medicine

This work was supported in part by a research grant of Samsung Biomedical Research Institute of Samsung Medical Center.

Address reprint requests to:
Yeon Hyeon Choe, MD, Department of Radiology and Center for Imaging Science, Samsung Medical Center, Sungkyunkwan University School of Medicine, 50 Ilwon-dong, Gangnam-Gu, Seoul 135-710, Korea.
Tel. (822) 3410-2509
Fax. (822) 3410-2559
e-mail: yhchoe@smc.samsung.co.kr

Objective: To evaluate the usefulness of multidetector-row computed tomography (CT) in the evaluation of reperfused myocardial infarction.

Materials and Methods: Eleven rabbits were subjected to 90-min occlusion of the left anterior descending coronary artery followed by reperfusion. Multidetector-row CT was performed 31 hours ±21 after the procedure and pre- and post-contrast multiphase helical CT images were obtained up to 10 min after contrast injection. The animals were sacrificed after 30 days and histochemical staining of the resected specimens was perfomed with 2'3'5-triphenyl tetrazolium chloride (TTC).

Results: In all 11 cases, the areas of myocardial infarction demonstrated with TTC-staining were identified on the CT images and the lesions showed hypoenhancement on the early phases up to 62 sec and hyperenhancement on the delayed phases of 5 min and 10 min compared with normal myocardial enhancement. The percentage area of the lesion with respect to the left ventricle wall on CT was significantly correlated with that of the TTC-staining results ($p < 0.001$ for both early and delayed phase CT) according to the generalized linear model analysis. The areas showing hypoenhancement on early CT were significantly smaller than those with hyperenhancement on delayed CT ($p < 0.0001$).

Conclusion: Multidetector-row CT may be useful in the detection and sizing of reperfused myocardial infarction.

The application of MRI to the diagnosis of ischemic heart disease has been extensively studied (1−3). This technique provides excellent tissue contrast between the normal and infarct tissue, especially on T2-weighted and contrast-enhanced T1-weighted images, as well as functional information. However, specific pulse sequences and hardware are required for cardiac imaging, and this makes MRI more time-consuming and expensive than CT. In emergency situations, patients with acute myocardial infarction may undergo CT, since their chest pain can mimic the symptoms of other diseases such as aortic dissection and pulmonary thromboembolism. Recently, high-speed CT scanners with multiple detector-rows have come to play a more important role in cardiac imaging than before. Although, several experimental studies have been published on the use of conventional CT in the evaluation of myocardial infarction (4−7), little information is available on the application of this new CT technology to the evaluation of acute myocardial infarction. A few clinical cases have been reported which included the CT findings of acute myocardial infarction (8, 9). This study was performed to test the reliability and usefulness of multidetector-row CT in the evaluation of myocardial infarction and reperfusion. This is one of the first attempts to evaluate myocardial

ischemia and reperfusion using multidetector-row CT in an experimental setting.

MATERIALS AND METHODS

Animal Experiment

The animal experiments were performed in accordance with our institutional guidelines. Eleven New Zealand white rabbits with a body weight of 2.8–3.7 kg were used. All rabbits were initially anesthetized with the intramuscular administration of 35 mg/kg ketamine and 5 mg/kg xylazine. Animals were intubated and anesthesia was induced with 4% enflurane and maintained throughout the surgical procedure with 2% enflurane. Initially, 0.2 mg/kg vecuronium was administered as a muscle relaxant and a 0.1 mg/kg/hr maintenance dose was infused into the ear vein during the operation. All rabbits underwent left lateral thoracotomy along the fourth or fifth intercostal space. The proximal one third of the left anterior descending coronary artery was ligated by a snare loop technique for 90 min. In one animal with a large first diagonal artery, this artery was ligated instead of the left anterior descending coronary artery. The snare loop was made with a 4–0 silk placed in a slender plastic tube. Subsequently, the coronary artery flow was restored and the chest wall was closed after aspiration of intrathoracic air and fluid.

Multislice CT

Multidetector-row CT was performed 31 hours ±21 (mean ±1 S.D.; range, 9–57 hours) after the initial procedure. Animals were placed in the left lateral decubitus position in the CT gantry. CT scanning was done from the cardiac base to the apex with the use of a four-slice helical CT (LightSpeed QX/I, GE Medical Systems, Milwaukee, Wis, U.S.A.). Multidetector-row CT was performed according to the following protocol: 3.75-mm slice thickness, 11.25 mm/sec table speed, high-quality mode (pitch of 3.0), 20-cm field-of-view, 50 mA, 120 kVp and 0.8-sec rotation speed. We chose rather thick CT slices, in order to be able to correlate the CT findings with the results of the histochemical staining by having almost the same slice thickness in both cases. Non-ionic contrast material (Iopamiro 300, Bracco, Milan, Italy) (3 mL/kg) was injected rapidly through the ear vein by hand. After precontrast scanning, postcontrast CT scans were performed. Ten series of images were obtained 10 sec after the contrast material injection, using an acquisition time of 3.6 sec and an interscan delay of 5 sec. Then, delayed images were obtained 5 min and 10 min after contrast injection. During CT scanning, the heart rates ranged from 150 to 220 beats/min and electrocardiography-gating was not applied due to the fast heart rates.

Histochemical Analysis

Each rabbit was sacrificed by means of an intravenous injection of ketamine and potassium chloride solution 28-35 days (average, 30 days) after the initial procedure, in order to determine the outcome of the area of CT-detected abnormality at 4 weeks. The heart was excised and cut into five or six 4-mm-thick consecutive slices along the short axes of the heart. At least one section was made through the presumed infarction center, which was also visible as a discolored area on observation of the excised heart. Then, the specimens were soaked in a 1.5% 2'3'5-triphenyl tetrazolium chloride (TTC) solution at 37°C and stained for 15 minutes (10). The area of myocardial infarction was defined as an area not stained with TTC. Then, the specimens were scanned at 400 dpi with a commercial scanner (Epson GT-9600 or Expression 1680 Pro, Seiko Epson Co.). We chose the image of the slice with maximal lesion size in each animal and calculated the percentage of the infarction area with respect to the total left ventricle wall area by using a commercially available software program (ALICE, Hayden Image Processing Solutions, Boulder, Colo, U.S.A.).

Image Analysis

All CT images and TTC specimen images were analyzed by two radiologists. For the estimation of interobserver and intraobserver variability, each radiologist analyzed the images independently twice, with a 1 month interval between each image analysis. We analyzed the visibility of the infarct areas showing abnormal contrast enhancement compared with that of the normal myocardium. The window level and width of the early phase images were set to 250/650-700 on the picture archiving and communication system workstation (PACS, PathSpeed Workstation, GE Medical Systems, Milwaukee, Wis). The window level and width of the delayed phase images were set to 150/100-150, in order to optimize the contrast of the lesions. After selecting the image that showed the maximal lesion size, we quantitatively measured the CT numbers of the lesion and the adjacent normal myocardium in each phase, by drawing a circle or freehand shape around the region-of-interest. The circle or freehand shape around the region-of-interest was made as large as possible (5–20 mm^2). The depth of involvement was classified into three grades: grade 1, involvement less than 1/3 of the left ventricle wall thickness; grade 2, between 1/3 and 2/3 of the wall thickness; and grade 3, more than 2/3 of the wall thickness. We independently calculated the area of myocardial infarction on each early and delayed CT image and pathologic

specimen twice. The area of abnormal contrast enhancement on the CT images and the area of infarct of the myocardium as observed with TTC-staining were expressed as a percentage of the area of the total left ventricular wall at the level with maximal lesion size. Inter- and intraobserver agreement in the calculation of the lesion size were measured by means of the intraclass correlation coefficient. Also, the correlation between the results of early-phase CT and histochemical staining, as well as the correlation between the results of delayed-phase CT and histochemical staining, were analyzed using the generalized linear model. To compare the sizes of the lesions on the early and delayed CT with those obtained from TTC-staining, a generalized linear model analysis was performed.

RESULTS

The reconstructed transverse CT images were close to being true short-axial images and were comparable to the TTC-stained slices of the specimens in all animals. In all 11 cases, the areas of myocardial infarction observed with TTC-staining were identified on the CT images and showed hypoenhancement on the early-phase and hyperenhancement on the delayed-phase images compared with that of the normal myocardium (Figs. 1, 2). The contrast between the lesions and the normal myocardium was most prominent at 10 sec on the early-phase images and equally prominent at 5 min and 10 min on the delayed-phase images. The quality of the CT images was adequate for image analysis in most cases, although low attenuation motion artifacts were found in the interventricular septum or other areas on one early CT image and on three delayed CT images. These artifacts could be differentiated from the true lesions, however, because they did not co-exist on the early and delayed CT images and because the demarcation of the low-density areas was not clear.

The depth of involvement on the early-phase CT images was grade 3 in eight cases and grade 1 (n=1) or 2 (n=2) with subendocardial involvement in three cases. The depth of involvement on the delayed-phase images was grade 3

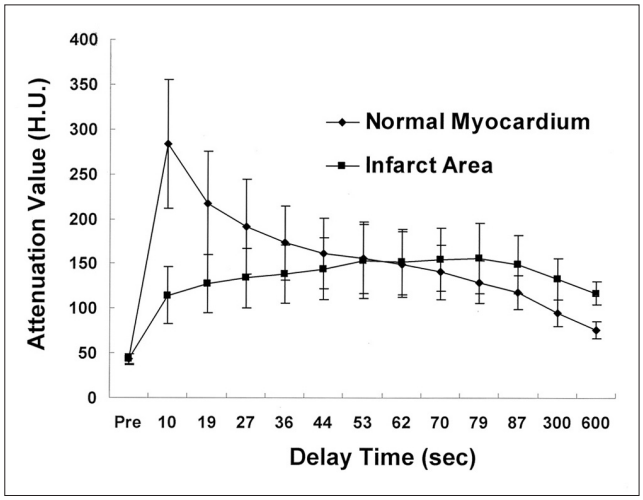

Fig. 2. Line graph of pooled data from all 11 rabbits shows enhancement patterns of normal myocardium and infarct myocardium on CT images. Infarct areas showed hypoenhancement at early phases and hyperenhancement at late phases compared with normal myocardium.

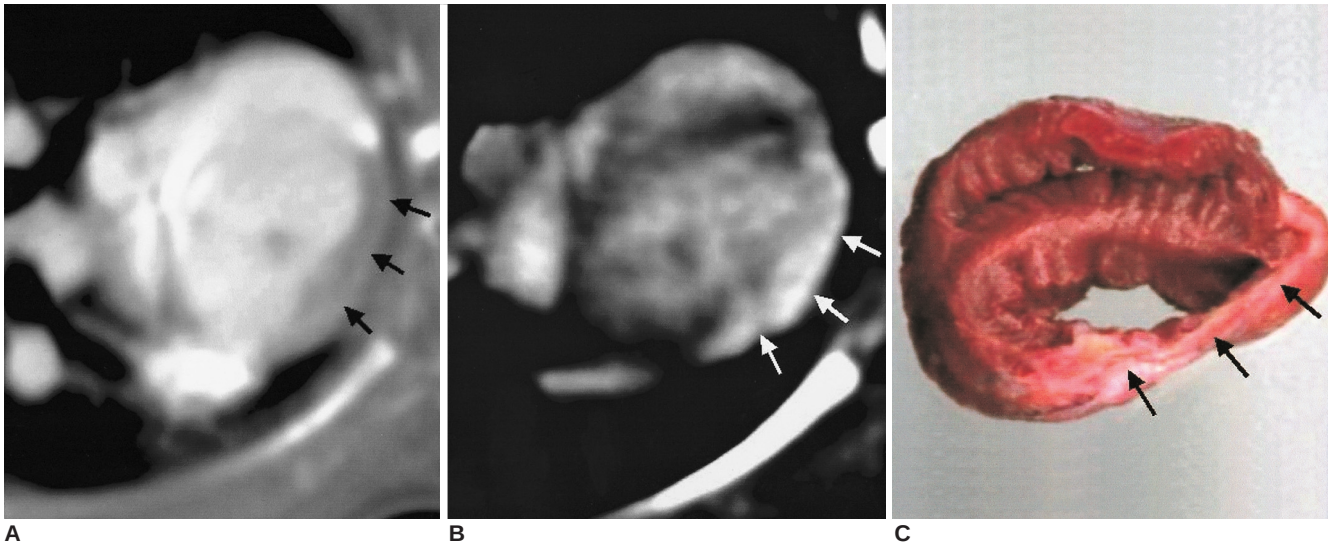

A **B** **C**

Fig. 1. Extensive myocardial infarction. Early-phase CT obtained at 27 sec following administration of contrast material (**A**) showed hypoenhancement (arrows) and 10-min-delayed image (**B**) showed hyperenhancement (arrows) in the anterior wall compared with normal myocardium. 2'3'5-triphenyl tetrazolium chloride-stained specimen obtained at four weeks after coronary artery occlusion and reperfusion (**C**) shows damaged myocardium (arrows) as a 2'3'5-triphenyl tetrazolium chloride-unstained area with wall thinning.

in nine cases and grade 1 (n=1) or 2 (n=1) with subendocardial involvement in two cases. The depth of involvement on the TTC-stained specimens was grade 3 in eight cases and grade 1 (n=1) or 2 (n=2) with subendocardial involvement in three cases. The depth of involvement on the early and delayed CT correlated well with that of TTC-stained specimens in ten animals, while one animal with grade 3 involvement on the delayed-phase CT showed grade 2 involvement on the TTC-stained specimens. Six animals (55%) had larger perfusion defects ($\geq$ 10% area) at early-phase CT and two of them with grade 3 involvement showed severe wall thinning on the TTC-stained specimens (thickness of the remaining wall < 1/2 of the normal myocardial thickness).

The percentage area of the lesion/left ventricle wall on the early and delayed CT was significantly correlated with that of the TTC-staining results [early-phase CT ($p < 0.001$), delayed-phase CT ($p < 0.001$)] in the generalized linear model analysis. There were good intra- and interobserver agreements for the early and delayed CT images and pathologic specimens (intraclass correlation coefficients > 0.80 for intraobserver reliability and intraclass correlation coefficients > 0.75 for interobserver reliability; Table 1). There was no significant difference in interobserver correlation between the early and delayed CT images ($p = 0.45$). However, there was a significant difference in the interobserver correlation between the TTC-stained specimens and the early and delayed CT images ($p < 0.05$).

The areas showing hypoenhancement on early CT were significantly smaller than those with hyperenhancement on delayed CT regardless of the observer ($p < 0.0001$). Both the areas showing hypoenhancement on early CT and those with hyperenhancement on delayed CT were larger than the infarct area identified with TTC-staining at four weeks, regardless of the observer ($p < 0.0001$).

DISCUSSION

Until now, the imaging techniques most commonly used for the evaluation of myocardial infarction have been echocardiography and radioisotope studies. The viability of the myocardium in the culprit arterial territory is an important issue. Stress echocardiography, single photon emission computed tomography with ^{201}Tl, and positron emission tomography with ^{18}F-deoxyglucose have been utilized to assess myocardial viability (11−15). However, it is difficult to accurately determine the extent of myocardial infarction due to the low image resolution of these techniques.

Contrast-enhanced MR imaging has been utilized for the evaluation of acute myocardial infarction (16−23). MR imaging using rapid imaging techniques and dedicated cardiac coils has demonstrated its usefulness in the detection of nonviable myocardium in patients with acute or chronic myocardial infarction, with better image resolution being obtained than in radionuclide studies. However, even with fast imaging techniques, the spatial resolution of MR imaging is still limited and the image matrix is typically 128×128 for a first-pass study and 256×192 or 256×160 for delayed-phase images with limited slice thickness. One advantage of MR imaging is the excellent tissue contrast obtained on T2-weighted and contrast-enhanced images, which assists in differentiating the damaged from the normal myocardium. Areas of hyperenhancement on 5- to 20-min-delayed images indicate damaged tissue with or without some overestimation of the extent of myocardial infarction (24−29).

Rogers et al. (30) found that lesions with hypoenhanced areas during first-pass studies did not improve in function. Hypoperfusion is due to a no-reflow phenomenon involving microvascular occlusion and edema in an area of myocardial infarction. Although this no-reflow zone has prognostic significance, the accurate estimation of its extent is sometimes difficult on perfusion MR imaging, because of the limited image resolution and the artifacts induced by respiration or chemical shifts. In our study, multidetector-row CT proved its usefulness in the detection of hypoperfused areas on early-phase images. The image resolution of CT (typically 512×512 matrix size with 20×20 cm field-of-view) is higher than that of MR imaging and the image contrast is sufficient for the differentiation of hypoperfused areas from the normal myocardium. In human applications, ECG-gated CT can reduce cardiac motion artifacts during the diastolic phase.

The detection of hyperenhanced areas necessitated the adjustment of the window level and width on PACS. The poor tissue contrast on the delayed images could be partly overcome by this technique. Delayed-phase images later than 10 min may not be necessary, because of the weak contrast between the lesion and the normal myocardium.

Table 1. Intraobserver and Interobserver Reliability in Interpretation of Early and Delayed-Phase CT and TTC-stained Specimens by Two Observers

	Intraobserver Reliability		Interobserver Reliability
	Observer 1	Observer 2	
Early CT	0.92	0.80	0.77
Delayed CT	0.89	0.92	0.76
TTC-Staining	0.96	0.96	0.97

Note.—Intra- and interobserver reliability were calculated using the intraclass correlation coefficient. TTC: 2'3'5-triphenyl tetrazolium chloride.

Therefore, an optimized multidetector-row CT protocol for myocardial infarction in rabbits would likely involve performing early-phase CT at 10 sec after contrast injection and delayed-phase CT at 5 –10 min.

The severity and extent of abnormalities and the contrast-enhancement patterns on the early and delayed CT correlated well with the four-week outcomes on the TTC-stained specimens. The difference in lesion size between the early and delayed CT reflects the reperfusion of the area at risk. Perfusion defects on early-phase CT result from microvascular occlusion. Hyperenhancement on delayed-phase CT may be ascribed to increased capillary permeability in the damaged myocardium and the subsequently prolonged stay of the contrast media in the infarct area (24, 26, 28 –30). The smaller size of the infarct observed with TTC-staining at 4 weeks compared with that on the CT images 1 day after the induced myocardial infarction suggests shrinkage of the damaged area and fibrosis (24).

CT equipment with a fast scanning time of around 0.4 sec is now available. Multidetector-row CT has shown its usefulness in the evaluation of coronary bypass grafts and in the imaging of native coronary arteries (31, 32). With the advent of 16-slice scanners, multidetector-row CT is expected to play a more important role in the evaluation of ischemic heart disease, by providing information on coronary arterial anatomy, ventricular function, myocardial perfusion, and viability.

The limitations of this study included cardiac motion artifacts and the limited number of slices on the CT imaging. Since the heart rates of the rabbits ranged from 150 to 220/min, ECG-gating was not applicable in this study. The axes of the pathologic specimens and those of the CT images were slightly different, because the hearts of the rabbits were positioned obliquely. However, in all rabbits, the hearts were always vertically oriented in the left-down decubitus position and the CT images were acquired in almost true short-axis planes. True short-axis cardiac images can be also reconstructed on a CT workstation.

The findings of our study indicate that the detection and evaluation of the size of the infarct area is feasible using multidetector-row CT. The images obtained using multidetector-row CT have adequate contrast for the detection of hypoenhanced areas in the first-pass studies of patients with acute myocardial infarction. The typical time course of acute myocardial infarction following contrast injection shows early hypoenhancement and delayed hyperenhancement compared with the normal myocardium. In conclusion, multidetector-row CT may be useful in the detection and evaluation of the extent of acute myocardial infarction.

Acknowledgement:

We wish to thank Jong Sung Kim, D.V.M., for the animal anesthesia, and Sun Woo Kim, Ph. D., for the statistical analysis.

References

1. McNarama MT, Tscholakoff D, Revel D, et al. Differentiation of reversible and irreversible myocardial injury by MR imaging with and without gadolinium-DTPA. *Radiology* 1986;158:765-769
2. Saeed M, Wendland MF, Takehara Y, Higgins CB. Reversible and irreversible injury in the reperfused myocardium: differentiation with contrast material-enhanced MR imaging. *Radiology* 1990;175:633-637
3. Pereira RS, Prato FS, Wisenberg G, Sykes J. The determination of myocardial viability using Gd-DTPA in a canine model of acute myocardial ischemia and reperfusion. *Magn Reson Med* 1996;36:684-693
4. Gray WR Jr, Parkey RW, Buja LM, et al. Computed tomography: in vitro evaluation of myocardial infarction. *Radiology* 1977;122:511-513
5. Hessel SJ, Adams DF, Judy PF, Fishbein MC, Abrams HL. Detection of myocardial ischemia in vitro by computed tomography. *Radiology* 1978;127:413-418
6. Higgins CB, Siemers PT, Schmidt W, et al. Evaluation of myocardial ischemic damage of various ages by computerized transmission tomography. Time-dependent effects of contrast material. *Circulation* 1979;60:284-291
7. Cipriano PR, Nassi M, Ricci MT, Reitz BA, Brody WR. Acute myocardial ischemia detected in vivo by computed tomography. *Radiology* 1981;140:727-731
8. Mochizuki T, Murase K, Higashino H, Koyama Y, Azemoto S, Ikezoe J. Demonstration of acute myocardial infarction by subsecond spiral computed tomography: early defect and delayed enhancement. *Circulation* 1999;99:2058-2059
9. Hilfiker PR, Weishaupt D, Marincek B. Multislice spiral computed tomography of subacute myocardial infarction. *Circulation* 2001;104:1083
10. Fishbein MC, Meerbaum S, Rit J, et al. Early phase acute myocardial infarct size quantification: validation of the triphenyl tetrazolium chloride tissue enzyme staining technique. *Am Heart J* 1981;101:593-600
11. Sicari R, Picano E, Landi P, et al. Prognostic value of dobutamine-atropine stress echocardiography early after acute myocardial infarction. Echo Dobutamine International Cooperative (EDIC) Study. *J Am Coll Cardiol* 1997;29:254-260
12. Williams MJ, Odabashian J, Lauer MS, Thomas JD, Marwick TH. Prognostic value of dobutamine echocardiography in patients with left ventricular dysfunction. *J Am Coll Cardiol* 1996;27:132-139
13. Phelps ME, Hoffman EJ, Selin C, et al. Investigation of [18F]2-deoxyglucose for the measure of myocardial glucose metabolism. *J Nucl Med* 1978;19:1311-1319
14. Burt RW, Perkins OW, Oppenheim BE, et al. Direct comparison of fluorine-18-FDG SPECT, fluorine-18-FDG PET and rest thallium-201 SPECT for detection of myocardial viability. *J Nucl Med* 1995;36:176-179
15. Kuijper AF, Vliegen HW, van der Wall EE, et al. The clinical impact of thallium-201 reinjection scintigraphy for detection of myocardial viability. *Eur J Nucl Med* 1992;19:783-789

16. Wesbey G, Higgins CB, Lanzer P, Botvinick E, Lipton MJ. Imaging and characterization of acute myocardial infarction in vivo by gated nuclear magnetic resonance. *Circulation* 1984;69: 125-130
17. Ratner RV, Okada RD, Newell JB, Pohost GM. The relationship between proton nuclear magnetic resonance relaxation parameters and myocardial perfusion with acute coronary arterial occlusion and reperfusion. *Circulation* 1985;71:823-828
18. Tscholakoff D, Higgins CB, McNamara MT, Derugin N. Early-phase myocardial infarction: evaluation by MR imaging. *Radiology* 1986;159:667-672
19. McNamara MT, Tscholakoff D, Revel D, et al. Differentiation of reversible and irreversible myocardial injury by MR imaging with and without gadolinium-DTPA. *Radiology* 1986;158:765-769
20. Peshock RM, Malloy CR, Buja LM, Nunnally RL, Parkey RW, Willerson JT. Magnetic resonance imaging of acute myocardial infarction: gadolinium diethylenetriamine pentaacetic acid as a marker of reperfusion. *Circulation* 1986;74:1434-1440
21. McNamara MT, Higgins CB, Ehman RL, Revel D, Sievers R, Brasch RC. Acute myocardial ischemia: magnetic resonance contrast enhancement with gadolinium-DTPA. *Radiology* 1984;153:157-163
22. Tscholakoff D, Higgins CB, Sechtem U, McNamara MT. Occlusive and reperfused myocardial infarcts: effects of Gd-DTPA on ECG-gated MR imaging. *Radiology* 1986;160:515-519
23. Wesbey GE, Higgins CB, McNarama MT, et al. Effect of gadolinium-DTPA on the magnetic relaxation times of normal and infarcted myocardium. *Radiology* 1984;153:165-169
24. Kim RJ, Fieno DS, Parrish TB, et al. Relationship of MRI delayed contrast enhancement to irreversible injury, infarct age, and contractile function. *Circulation* 1999;100:1992-2002
25. Choi SI, Jiang CZ, Lim KH, et al. Application of breath-hold T2-weighted, first-pass perfusion and gadolinium-enhanced T1-weighted MR imaging for assessment of myocardial viability in a pig model. *J Magn Reson Imaging* 2000;11:476-480
26. Saeed M, Bremerich J, Wendland MF, Wyttenbach R, Weinmann HJ, Higgins CB. Reperfused myocardial infarction as seen with use of necrosis-specific versus standard extracellular MR contrast media in rats. *Radiology* 1999;213:247-257
27. Arheden H, Saeed M, Higgins CB, et al. Reperfused rat myocardium subjected to various durations of ischemia: estimation of the distribution volume of contrast material with echo-planar MR imaging. *Radiology* 2000;215:520-528
28. Schaefer S, Malloy CR, Katz J, et al. Gadolinium-DTPA-enhanced nuclear magnetic resonance imaging of reperfused myocardium: identification of the myocardial bed at risk. *J Am Coll Cardiol* 1988;12:1064-1072
29. Saeed M, Lund G, Wendland MF, Bremerich J, Weinmann H, Higgins CB. Magnetic resonance characterization of the peri-infarction zone of reperfused myocardial infarction with necrosis-specific and extracellular nonspecific contrast media. *Circulation* 2001;103:871-876
30. Rogers WJ Jr, Kramer CM, Geskin G, et al. Early contrast-enhanced MRI predicts late functional recovery after reperfused myocardial infarction. *Circulation* 1999;99:744-750
31. Willmann JK, Szente-Varga M, Roos JE, Hilfiker PR, Weishaupt D. Three-dimensional images of extra-anatomic arterial bypass graft using multidetector row spiral computed tomography data with volume rendering. *Circulation* 2001;104:E154-155
32. Budoff MJ, Achenbach S, Duerinckx A. Clinical utility of computed tomography and magnetic resonance techniques for noninvasive coronary angiography. *J Am Coll Cardiol* 2003;42: 1867-1878